Article

Planar Tetracoordinate Carbon in Extended Systems

Pattath D. Pancharatna, Miguel Angel Mndez-Rojas, Gabriel Merino, Alberto Vela, and Roald Hoffmann

J. Am. Chem. Soc., **2004**, 126 (46), 15309-15315• DOI: 10.1021/ja046405r • Publication Date (Web): 02 November 2004

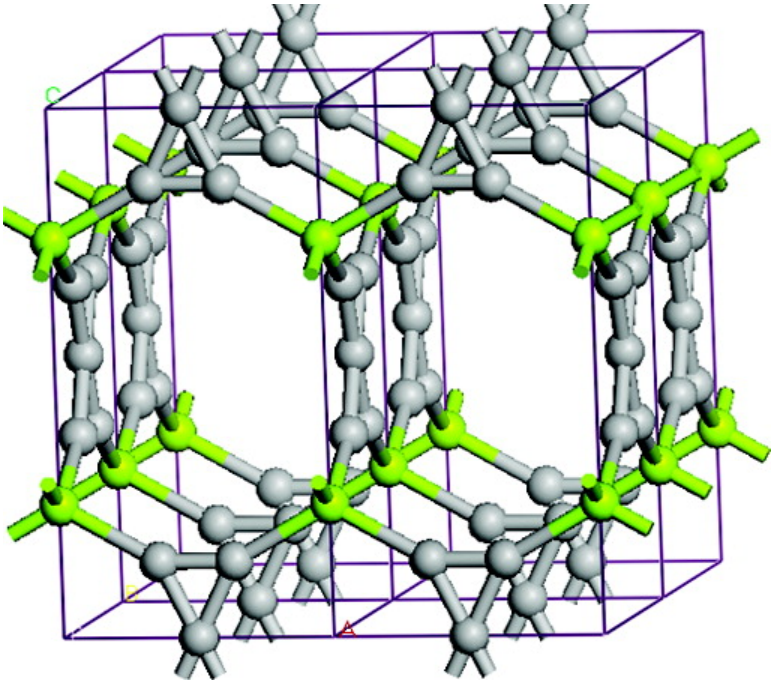

J|A|C|S
ARTICLES
Published on Web 11/02/2004

Planar Tetracoordinate Carbon in Extended Systems

Pattath D. Pancharatna,[†] Miguel Angel Méndez-Rojas,*[,‡] Gabriel Merino,[§] Alberto Vela,[||] and Roald Hoffmann*[,†]

Contribution from the Department of Chemistry and Chemical Biology, Cornell University, Ithaca, New York 14853; Departamento de Química y Biología, Universidad de las Américas-Puebla, Ex-Hda de Sta. Catarina Mártir, A. P. 100, Cholula 72820, Puebla, México; Institut für Physikalische Chemie und Elektrochemie, TU Dresden, D-01062 Dresden, Germany; and Departamento de Química, Centro de Investigación y de Estudios Avanzados A. P. 14-740, México, D.F., 07000, México

Received June 17, 2004; E-mail: rh34@cornell.edu

Abstract: A recently proposed system with a central planar tetracoordinate carbon linking two three-membered rings, C_5^{2-}, lends itself to extension in one, two, and three dimensions. Our construction of potential realizations begins with an analysis of the electronic structure of C_5^{2-}. Dimers such as $C_{10}Li_3^-$, $C_{10}Li_4$, and a trimer $C_{15}Li_6$ are then examined, and their geometries are optimized to find clues for ways the C_5^{2-} unit may polymerize in the presence of countercations. Coordination through the terminal carbons is favored in the oligomers and polymers; several electronically and structurally reasonable systems of the stoichiometry C_5M_x (M = Li, $x = 2$; M = Be, Pt, Zn, $x = 1$) emerge from band structure calculations and energetic considerations.

Introduction

Stabilization of planar tetracoordinate carbon (C_{pt}) continues to be a fascinating experimental and theoretical challenge.[1−11] For a C_{pt} surrounded by four other carbons, the simplest molecule that (so far on paper, or rather in silico) achieves this goal is C_5^{2-}.[12] Its metastability is a consequence of the delocalization of the electrons in the p orbital of the central carbon.[13] The possibility of an extended network based on motifs containing a C_{pt} surrounded by other elements has been explored previously.[14−16] The C_5^{2-} system appears to be a good starting point for exploring polymeric forms containing C_{pt}, which is the focus of this paper.

Computational Methodology

The geometry optimizations of the discrete molecular systems (C_5Li_2, $C_5Li_4^{2+}$, $C_{10}Li_3^-$, $C_{10}Li_4$, $C_{15}Li_6$) reported in this paper are performed using Gaussian 98.[17] Structures are optimized using Becke's exchange (B), Lee, Yang, and Parr (LYP) correlation, and the hybrid functional (B3LYP) approach,[18,19] as implemented in the Gaussian set of programs. All the molecular calculations are done with the 6-311++G(2d) basis set.[20] Calculations have been performed on various extended networks of C_5M_x (M = Li, $x = 2$; M = Pt, Zn, Be, $x = 1$) using the extended Hückel (EH) based YAeHMOP program to verify the stoichiometry.[21] A special case of C_5Zn where Zn and the C_{pt} are interchanged in positions is also considered. For geometry optimization of the extended models, the density functional theory (DFT) based VASP program is used.[22−25] The ultrasoft pseudopotentials employed in VASP are based on the projector-augmented-wave (PAW) method.[26] The Perdew−Wang 91 (PW91) functional within the generalized

[†] Cornell University.
[‡] Universidad de las Américas-Puebla.
[§] TU Dresden.
[||] Centro de Investigación y de Estudios Avanzados.

(1) Hoffmann, R.; Alder, R. W.; Wilcox, C. F. *J. Am. Chem. Soc.* **1970**, *92*, 4992.
(2) Sorger, K.; Schleyer, P. v. R. *THEOCHEM* **1995**, *338*, 317.
(3) Siebert, W.; Gunale, A. *Chem. Soc. Rev.* **1999**, *28*, 367.
(4) Minkin, V. I.; Minyaev, R. M.; Hoffmann, R. *Usp. Khim.* **2002**, *71*, 989.
(5) Radom, L.; Rasmussen, D. R. *Pure Appl. Chem.* **1998**, *70*, 1977.
(6) Rottger, D.; Erker, G. *Angew. Chem., Int. Ed. Engl.* **1997**, *36*, 813.
(7) Keese, R. *Chimia* **1982**, *36*, 300.
(8) McGrath, M. P.; Radom, L. *J. Am. Chem. Soc.* **1993**, *115*, 3320.
(9) Rasmussen, D. R.; Radom, L. *Angew. Chem., Int. Ed.* **1999**, *38*, 2876.
(10) Wang, Z. X.; Schleyer, P. v. R. *J. Am. Chem. Soc.* **2002**, *124*, 11979.
(11) Priyakumar, U. D.; Reddy, A. S.; Sastry, G. N. *Tetrahedron Lett.* **2004**, *45*, 2495.
(12) Merino, G.; Mendez-Rojas, M. A.; Vela, A. *J. Am. Chem. Soc.* **2003**, *125*, 6026.
(13) Merino, G.; Mendez-Rojas, M. A.; Beltran, H. I.; Corminboeuf, C.; Heine, T.; Vela, A. **2004**, in press. This paper discusses in detail alternative geometries for C_5^{2-}.
(14) Merschrod, E. F.; Tang, S. H.; Hoffmann, R. *Z. Naturforsch., B* **1998**, *53*, 322.
(15) Li, X.; Zhang, H. F.; Wang, L. S.; Geske, G. D.; Boldyrev, A. I. *Angew. Chem., Int. Ed.* **2000**, *39*, 3630.
(16) Geske, G. D.; Boldyrev, A. I. *Inorg. Chem.* **2002**, *41*, 2795.
(17) Frisch, M. J.; Trucks, G. W.; Schlegel, H. B.; Scuseria, G. E.; Robb, M. A.; Cheeseman, J. R.; Zakrzewski, V. G.; Montgomery, J. A.; Stratmann, R. E.; Burant, J. C.; Dapprich, S.; Millan, J. M.; Daniels, A. D.; Kudin, K. N.; Strain, M. C.; Farkas, O.; Tomasi, J.; Barone, V.; Cossi, M.; Cammi, R.; Mennucci, B.; Pomelli, C.; Adamo, C.; Clifford, S.; Ochterski, J.; Petersson, G. A.; Ayala, P. Y.; Cui, Q.; Morokuma, K.; Malick, D. K.; Rabuck, A. D.; Raghavachari, K.; Foresman, J. B.; Cioslowski, J.; Ortiz, J. V.; Baboul, A. G.; Stefanov, B. B.; Liu, G.; Liashenko, A.; Piskorz, P.; Komaromi, I.; Gomperts, R.; Martin, R. L.; Fox, D. J.; Keith, T.; Al-Laham, M. A.; Peng, C. Y.; Nanayakkara, A.; Gonzales, C.; Challacombe, M.; Gill, P. M. W.; Johnson, B.; Chen, W.; Wong, M. W.; Andreas, J. L.; Head-Gordon, M.; Reploge, E. S.; Pople, J. A. *Gaussian 98*, revision A7 ed.; Gaussian Inc: Pittsburgh, PA, 1998.
(18) Becke, A. D. *J. Chem. Phys.* **1993**, *98*, 5648.
(19) Lee, C. T.; Yang, W. T.; Parr, R. G. *Phys. Rev. B* **1988**, *37*, 785.
(20) Krishnan, R.; Binkley, J. S.; Seeger, R.; Pople, J. A. *J. Chem. Phys.* **1980**, *72*, 650.
(21) Landrum, G. A.; Glassy, W. V.; YAeHMOP 3.01 (available free at http://yaehmop.sourcefroge.net).
(22) Hohenberg, P.; Kohn, W. *Phys. Rev. A* **1964**, *136*, 864.
(23) Kresse, G.; Hafner, J. *Phys. Rev. B* **1993**, *47*, 558.
(24) Kresse, G.; Hafner, J. *Phys. Rev. B* **1994**, *49*, 558.
(25) Kresse, G.; Furthmüller, J. *Comput. Mater. Sci.* **1996**, *6*, 15.
(26) Kresse, G.; Hafner, J. *Phys. Rev. B* **1999**, *59*, 1758.

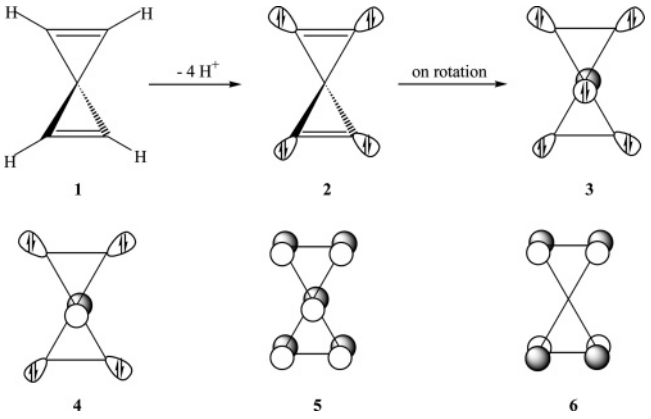

Figure 1. Simplified picture of the construction of the MOs (**4**, **5**, **6**) of C_5^{2-} from C_5^{4-} (**2**) derived from C_5H_4 (**1**). **3** is the intermediate C_5^{4-} in a planar geometry.

gradient approximation (GGA) is used to treat the exchange-correlation energy.[27−29] A cutoff energy of 500 eV and an energy convergence of 1.0e−07 eV atom^{-1} are used. For the crystal lattice, integration over the symmetrized Brillouin Zone is performed using the k-points generated via the Monkhurst−Pack scheme.[30] In all systems, for the generation of the mesh a uniform k-point separation of 2 pm^{-1} is employed. The geometry is well converged with respect to the plane-wave energy cutoff and k-point sampling.

Why C_5^{2-}?

One way to describe simply the MOs of C_5^{2-} and why it features a C_{pt} is to start with a spiropentadiene, **1** (Figure 1). Four protons can be formally removed from C_5H_4, **1**, to obtain C_5,$^{4-}$ **2**. This generates four lone pairs, one on each terminal carbon (C_t) and pointing outward, roughly in the direction where the hydrogen nuclei were located in **1**. Rotating one cyclopropenyl ring against the other, to put all five carbons into one plane, results in planar C_5,$^{4-}$ **3**. The central π-type lone pair, a characteristic feature of square planar carbon systems, will be surely destabilized. Vacating this MO will result in C_5^{2-}, **4**, for which there are four out-pointing lone pairs and a π-system of two occupied orbitals, which must be **5** and **6** (schematic).

In a second approach, Figure 2 constructs the molecular orbitals (MOs) of C_5^{2-} from the interaction of four C_t's with the central C_{pt}. The energy level positions come from an extended Hückel (EH) calculation[31] on a DFT-optimized geometry of the C_5^{2-} molecule. The colors distinguish the MO symmetries. Those MOs which contain no contribution from the C_{pt} by symmetry are assigned black. The σ MOs emphasize the radial and tangential p orbital origins.

The four localized lone pairs of **4** (Figure 1) should transform as $a_g + b_{1u} + b_{2u} + b_{3g}$. Their delocalized equivalents are to be found in $1b_{2u}$, b_{3g}, $2a_g$, and $2b_{1u}$ of Figure 2. Two very low-lying MOs (a_g and b_{1u}) with mainly s character are omitted in the diagram. The destabilization of $2a_g$ and $2b_{1u}$ (mostly bonding) over $1b_{2u}$ and b_{3g} (mostly antibonding) is due to the second-order interaction with the σ set of MOs. Since these radial MOs mix with the tangential MOs ($1a_g$, $1b_{1u}$, and

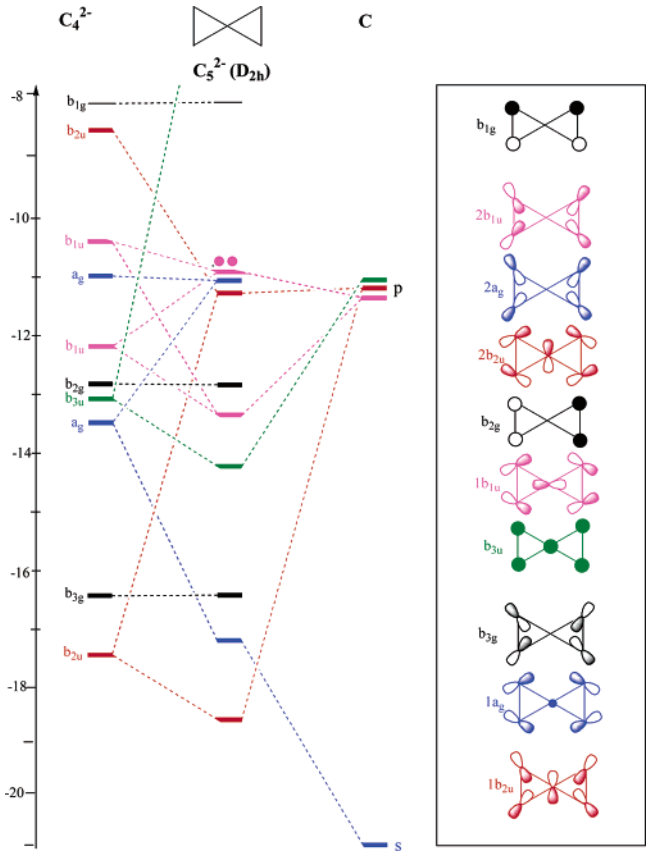

Figure 2. Correlation diagram between the four C_t and the central C_{pt} generating the MOs of C_5^{2-}. The bold and thin lines differentiate between the filled and empty levels.

$2b_{2u}$) due to their common symmetry, the orientation of the canonical orbitals differs slightly from those shown schematically in Figure 2. The *p* orbitals perpendicular to the plane, which are involved in the formation of π MOs, are shown as circles, symbolizing their "top" (above the plane) phase. The two π MOs **5** and **6** (Figure 1) are identified as b_{3u} and b_{2g} in Figure 2. The corresponding antibonding combination lies even above the LUMO (b_{1g}).

Discrete systems

Countercations are used to further stabilize the system (C_5^{2-}). Calculations on C_5^{2-} using two Li^+ ions to balance the charge result in three different isomers of C_5Li_2 (**7**−**9**, Figure 3) distinguished by the position of Li ions. The calculated energies of **7**−**9** indicate that the metal ions prefer coordinating the carbons not linked to each other.

To understand the arrangement of four Li^+ ions around a C_5^{2-} unit, two isomers were explored (**10** and **11**, Figure 3). In this case, isomer **10** is found to be more stable than **11** by 51.4 kJ mol^{-1}. **10** maximizes the electrostatic interactions between the lone pairs at the four C_5^{2-} corners and the four Li^+ ions and is the one dictated by two of the three highest lying occupied MOs ($2b_{1u}$ and $2a_g$) of C_5^{2-} (see Figure 2).

The design of a fragment containing two C_5^{2-} units (a dimer) would require including four monocations (Li^+) in order to keep the electroneutrality of the system. The relative stabilities of the monomers give an idea of how to arrange the metal ions around the C_5 unit. The most stable isomer in the C_5Li_2 series calculated here[32] (**7**) suggests two possible arrangements for a

(27) Perdew, J. P.; Wang. Y. *Phys. Rev. B* **1986**, *33*, 8800.
(28) Perdew, J. P. *Electronic Structure of Solids*; Ziesche, P., Eschrig, H., Eds. Akademie Verlag: Berlin, 1991; p 11
(29) Payne, M. C.; Teter, M. P.; Allan, D. C.; Arias, T. A.; Joannopoulos, J. D. *Rev. Mod. Phys.* **1992**, *64*, 1045.
(30) Monkhost, H. J.; Pack, J. *Phys. Rev. B.* **1976**, *13*, 5188.
(31) Hoffmann, R. *J. Chem. Phys.* **1963**, *39*, 1397.

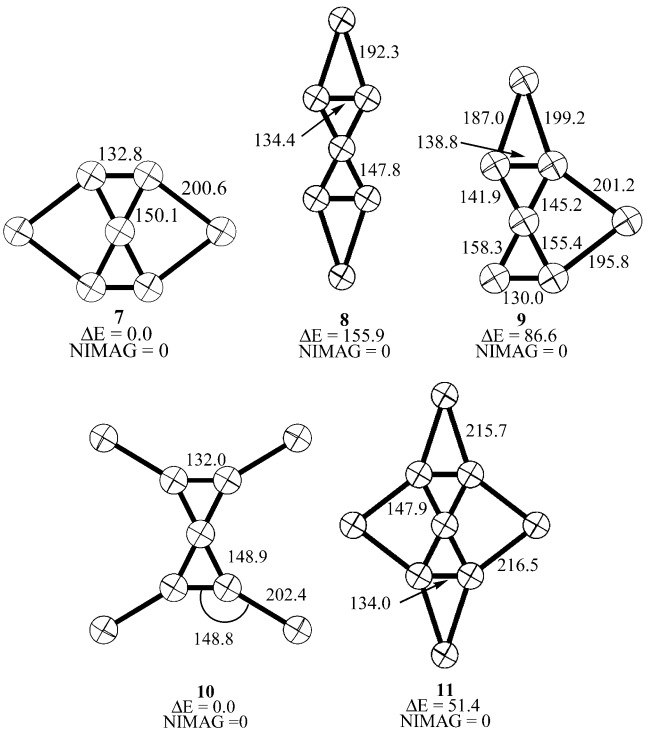

Figure 3. Possible isomers (**7**−**9**) of C_5Li_2 and (**10** and **11**) of $C_5Li_4^{2+}$ with varying metal positions are shown. ΔE is the relative energy (in kJ mol^{-1}) with respect to the most stable isomers **7** and **10** of C_5Li_2 and $C_5Li_4^{2+}$, respectively. All these structures are local minima on the PES as observed from the number of imaginary frequencies (NIMAG).

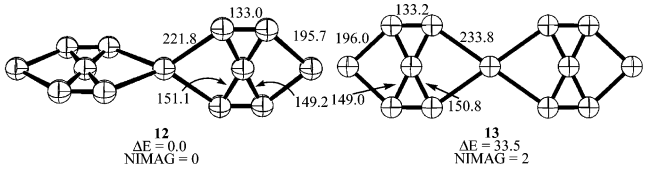

Figure 4. Two possible isomers (**12** and **13**) of $C_{10}Li_3^-$ with perpendicular and coplanar C_5^{2-} units. ΔE is the relative energy (in kJ mol^{-1}) with respect to **12**.

$C_{10}Li_3^-$ dimer; one where both C_5^{2-} units are perpendicular to each other, **12**, and another, where the units are coplanar, **13** (Figure 4). Structure **12** is a minimum on the potential energy surface (PES), while **13** has two imaginary frequencies.

The most stable structure **10** in the $C_5Li_4^{2+}$ series leads to a dimer $C_{10}Li_4$ (**14**, Figure 5). In the optimized structure, two of the Li^+ ions occupy positions between the terminal carbons which are not linked to each other. To gain further insight on the preferred position of the metal, a trimer $C_{15}Li_6^{2-}$ **15** (Figure 5) is also constructed; it continues the bonding motif found for **10**. Both **14** and **15** are minima on their PES. These results provide clues for extending the system in two and three dimensions.

Extended Networks based on C_5^{2-}

Based on the results in the previous section, different 1-D and 2-D networks can be constructed. The stable dimers **12** and **14**, as well as structure **13**, lend themselves to extension to 1-D chains of C_5 units. These polymeric chains are depicted in Figure 6 as **I**, **II**, and **III**, respectively. Since the ratio of a C_5 unit to

(32) There may be other more stable C_5Li_2 isomers with a nonsquare-planar carbon (see ref 13).

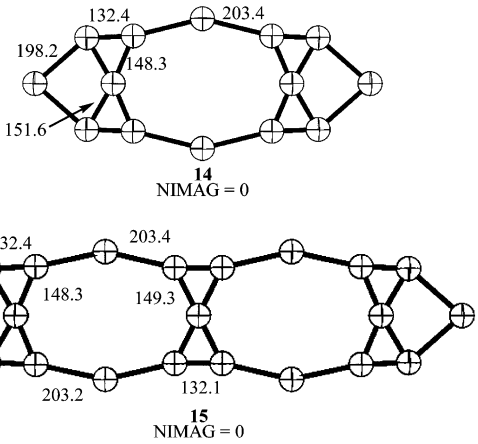

Figure 5. Optimized structures of $C_{10}Li_4$ and $C_{15}Li_6$.

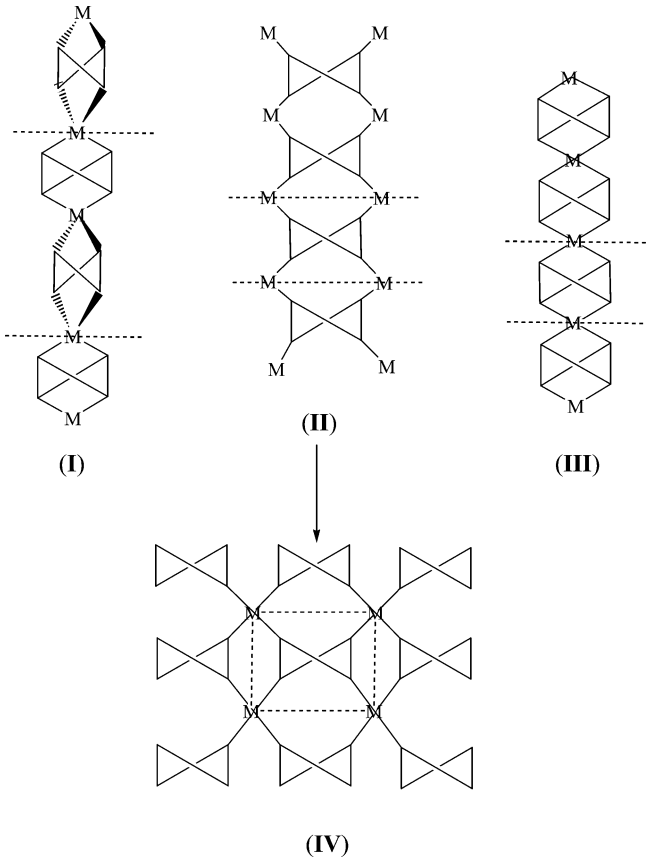

Figure 6. Schematic diagram for a 1-D (**I**, **II**, **III**) and a 2-D (**IV**) pattern of C_5^{2-} units bridged by appropriate metal ions.

the metal in a unit cell of **I** and **III** is 1:1, a divalent metal ion is needed to compensate for the 2− charge on C_5. **II** involves a 1:2 ratio of C_5 to metal, which might be supported by Li^+ ions. If Li^+ is replaced by a divalent tetracoordinate metal ion, **II** can be converted into a 2-D network, as shown in **IV**, Figure 6. The repeating units are shown by dashed lines.

Since **I** involves a tetrahedral coordination around the metal and the requirement of a divalent metal ion, a Zn^{2+} or Be^{2+} ion can be chosen for building the network. The choice of Zn and Be is based on the existence of systems containing $(Zn/Be)^{2+}$ with a tetrahedral arrangement, for e.g., $Zn(CN)_2$ and CBe_2.[33,34] In the case of **II**, Li^+ ions are retained, as in structures **14** and **15**, whereas, for **III**, platinum might be a good choice,

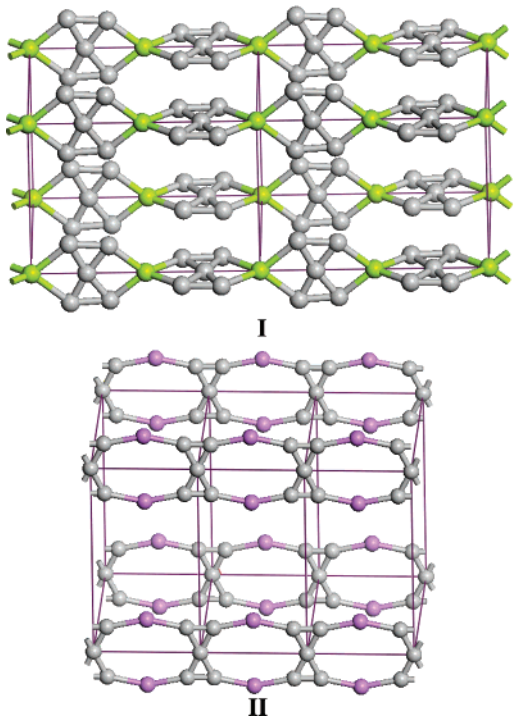

Figure 7. Optimized lattice of (**I**) C_5Zn and (**II**) C_5Li_2.

Table 1. Space Group, *Z*, Cell Parameters (*a*, *b*, *c* in Å), and *V* (Volume in Å^3) of the Different C_5M_x Systems Are Given

system	space group	*Z*	*a*	*b*	*c*	*V*
C_5Zn (**I**)	*P*42/*mmc*	2	9.90	9.90	9.33	915.14
C_5Li_2	*Pmmm*	1	5.33	9.91	9.97	526.80
C_5Pt	*Pmmm*	1	3.84	4.46	5.22	89.32
C_5Zn (**V**)	*P*42/*mmc*	2	4.76	4.76	9.14	206.56
C_5Be	*P*42/*mmc*	2	4.45	4.45	8.82	174.83
C_5Zn (**VII**)	*P*42/*mmc*	2	3.78	3.78	10.53	150.46
C_5Ni	*P*42/*mmc*	2	3.82	3.82	10.44	152.04

as it often exists in a square planar arrangement with an oxidation state of II.[35] The 2-D network of **IV** might be realized with Pt as metal ions as well. While the results from the studies on molecular systems showed two most preferred positions for metal ions, (i.e., either bonding the C_ts or connecting two C_ts which are not bonded to each other), the two polymorphic forms of C_5Pt (**III** and **IV**) will enable one to say which among these two provides the most stable site for the metal ions.

Phase **I** is found to be stable with Zn; C_5Be failed to converge. C_5Zn (**I**) and C_5Li_2 (**II**) are optimized in a 3-D lattice, and the resulting geometries are shown in Figure 7. C_5Be (**I**) has a tetragonal unit cell (space group *P*42/*mmc*), while **II** has an orthorhombic unit cell (space group *Pmmm*).

The optimized lattice parameters of **I** are given in Table 1. Due to the difficulty VASP has in dealing with 1-D systems, a 3-D system is used with the discrete chains well separated from each other (as can be seen from the cell parameters of ~1000 pm for *a* and *b* in Table 1). The large separation is retained even after convergence, which essentially implies that the system

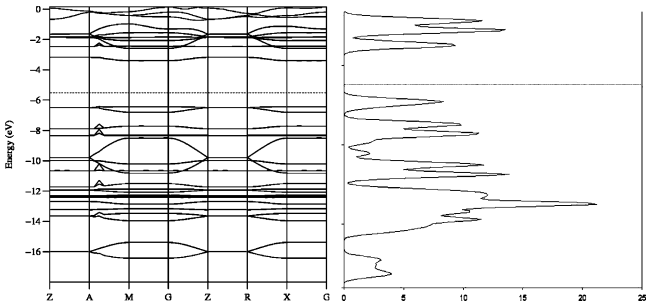

Figure 8. Band structure and total DOS for optimized C_5Zn (**I**).

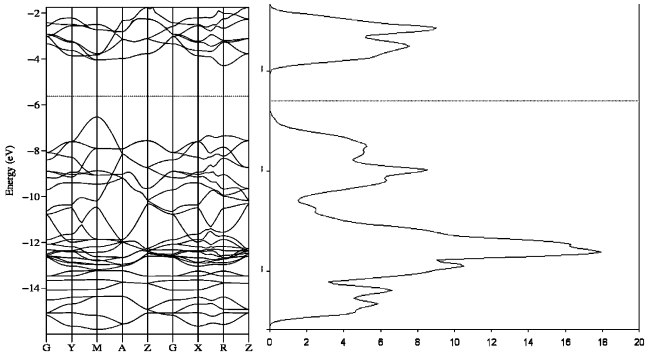

Figure 9. Band structure and total DOS of optimized C_5Li_2.

wants to remain one-dimensional. The DFT based band structure and total DOS for **I** are shown in Figure 8.

The C−C bond lengths within the C_5^{2-} unit of **I** closely resemble the values calculated for the corresponding dimer, $C_{10}Li_3^-$ (**12**); the bond lengths range from 135 to 149 pm. In general the C_t-C_t bonds tend to be shorter compared to the C_t-C_{pt} bond in all the systems studied here. The extent of shortening of the C_t-C_t bond can be correlated to the back-donation from C_{pt}. Thus the terminal C_t-C_t bond (133 pm) which can be related to an acetylenic bond, is disturbed by partial back-donation from the central C_{pt} to one of the π^*-bonds (in-plane) of C_t-C_t. The MOs which contain contributions from the in-plane π and π^*-MOs of C_t-C_t emerge as the tangential MOs in C_5^{2-}, $1a_g$, $1b_{1u}$, and $2b_{2u}$ as seen in Figure 2. Here $2b_{2u}$, which is antibonding between C_t, can be identified as involving back-donation from C_{pt} to the in-plane π^* of C_t-C_t and contributes to some extent to the elongation of the C_t-C_t bond. The $Zn-C_t$ and $Zn-C_{pt}$ distances are 212 and 233 pm, respectively.

In C_5Li_2, the geometrical parameters are not very different from the calculated dimer (**14**) and trimer (**15**). The optimized unit cell dimensions are given in Table 1. The C−C bonding distance within the C_5 unit ranges from 133 to 150 pm. In the optimized lattice, the discrete chains remain separated from each other by ~1000 pm (see *b* and *c* values in Table 1). The calculated band structure and DOS obtained from VASP for C_5Li_2 are shown in Figure 9; the band gap is ~3 eV. The bands are almost flat, as the interactions with the Li atoms binding the C_5 units are almost negligible.

C_5Pt in a 3-D lattice is optimized in an orthorhombic unit cell, space group *Pmmm* (Figure 10). On geometry optimization, **III** actually went over to **IV**, proving that the metal prefers to stay entirely bonded to the C_t atoms of the C_5 unit, one among the two possibilities found by calculations on the discrete systems. This is also reflected in the relative stabilities of the

(33) Hoskins, B. F.; Robson, R. *J. Am. Chem. Soc.* **1990**, *112*, 1546.
(34) Lee, C. H.; Lambrecht, W. R. L.; Segall, B. *Phys. Rev. B* **1995**, *51*, 10 392.
(35) Collmann, J. P.; Hegedus, L. S.; Norton, J. R.; Finke, R. G. *Principles and Applications of Organotransition Metal Chemistry*; University Science Books: Mill Valley, CA, 1987.

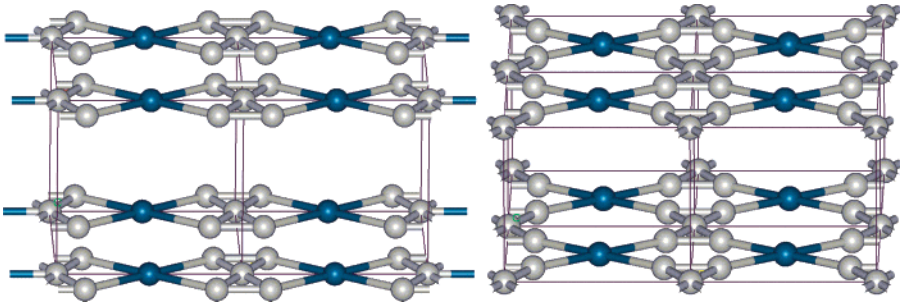

Figure 10. 3-D unit cells of the **III** and **IV** forms of C_5Pt are shown. **III** correspond to the initial geometry and **IV** to the relaxed structure.

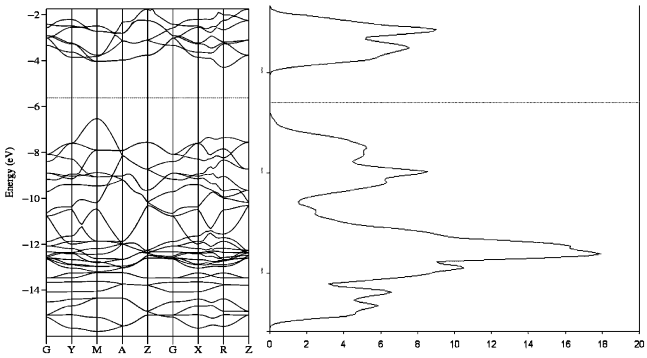

Figure 11. Calculated bands and total DOS of the optimized C_5Pt system.

isomeric forms of $C_5Li_4^{2+}$, with **10** being more stable than **11** by 51.4 kJ mol^{-1}. The transformation may be viewed as the migration of Pt from the edge (*b* axis) in **III** to the face in **IV**, along the *c* axis.

The optimized unit cell dimensions for **IV** are given in Table 1. The nonbonding distances between the C_t atoms of the neighboring units are 314 and 254 pm along the *b* and *c* axes, respectively. Hence, the C_5 units are well-isolated from each other and are connected only through the bridging Pt ion. The C−C distances within the C_5 unit reproduce the trend observed in its molecular analogues (C_t-C_t 132.0 pm, C_t-C_{pt} 149 pm). Though Pt maintains a planar arrangement, the ligands are not at the corners of a square; the calculated C_t-Pt-C_t bond angles are 102° (*b* axis) and 78° (*c* axis), respectively.

The band structure and the total density of states (DOS) for **IV** are given in Figure 11. A band gap of ∼1 eV indicates semiconducting behavior.

Based on the above observation regarding the preferred position of metal ions, a 3-D network is designed with Zn/Be (**V**, **VI**) connecting the C_5 units by bridging through the C_t atoms. Figure 12 gives the unit cell of C_5M (M = Zn, Be); the C_5 units run along the *a* and *b* axes, and the metal connecting them adopts a tetrahedral environment. The structure is tetragonal and belongs to space group *P*42/*mmc*. The essential parameters of the optimized system are given in Table 1.

The computed bond lengths of Zn−C and Be−C are in close agreement with the known systems ($Zn-C_2N_2$ = 192 pm and $Zn-C_5$ = 197 pm, Be_2-C = 188 pm and $Be-C_5$ = 179 pm). The nonbonding C_t-C_t distances, same along the *a* and *c* axes by symmetry, are 344 and 313 pm for Zn and Be systems, respectively. The geometry of the C_5 unit does not deviate from the values calculated earlier, with normal C_t-C_t [131.6 (Zn) and 132 (Be)] and C_t-C_{pt} [147 (Zn) and 148 (Be)] distances. The angles around Zn and Be deviate from a perfect tetrahedron,

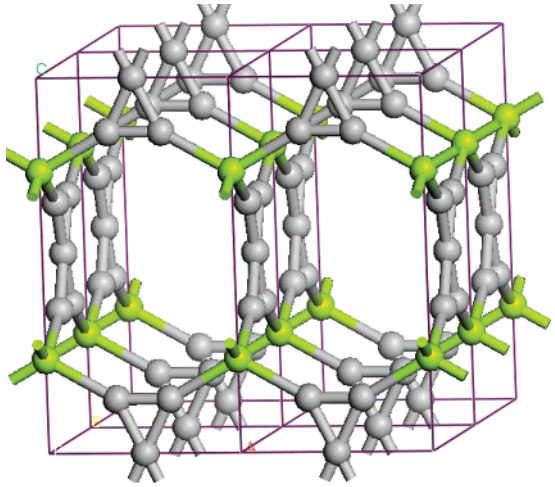

V/VI

Figure 12. Unit cell of a 3-D network of C_5M (M = Zn, Be).

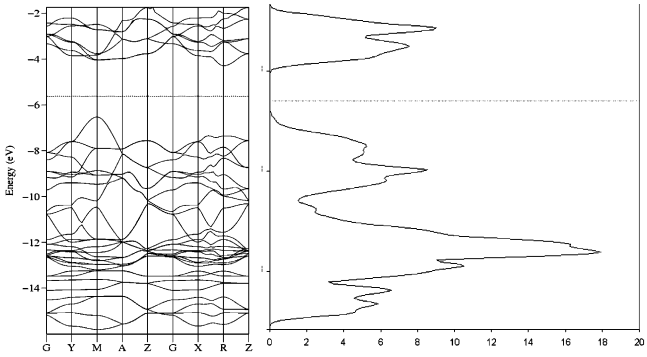

Figure 13. Calculated bands and total DOS of optimized C_5Zn.

with values of around 121° (between atoms along the same axes) and 104° (between two different axes).

The band structure and total DOS for C_5Zn are given in Figure 13. This system and the analogous Be one (calculated, but details are not shown here) have a band gap of ∼2−3 eV, indicating insulating behavior. The band structure of the Be phase (not shown in detail here) exhibits similar features especially near the Fermi level. The bands in the region of 11−14 eV in C_5Zn are the d-band of Zn. A detailed analysis, not shown in the figure, indicates a small participation of Zn 3d levels and slightly stronger bonding in Zn−C than Be−C.

ZnC_5 (**V**) is polymorphic to the already calculated system **I**. **V** is found to be more stable than **I** by 685 kJ mol^{-1} per ZnC_5, further suggesting the greater preference of the metal ion to bond exclusively to the C_t atom of C_5^{2-} unit.

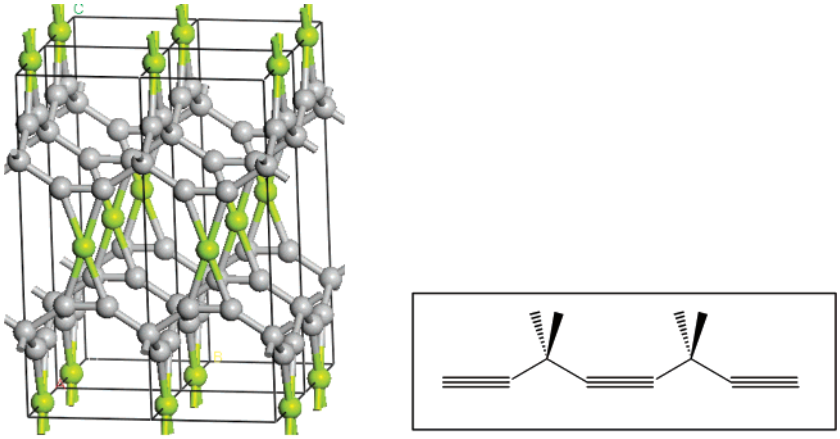

VII

Figure 14. Unit cell of C_5M **(VII)** with M at the square planar and C at the tetrahedral positions. The inset shows the skeleton of the carbon chain running along the *a* and *b* axes.

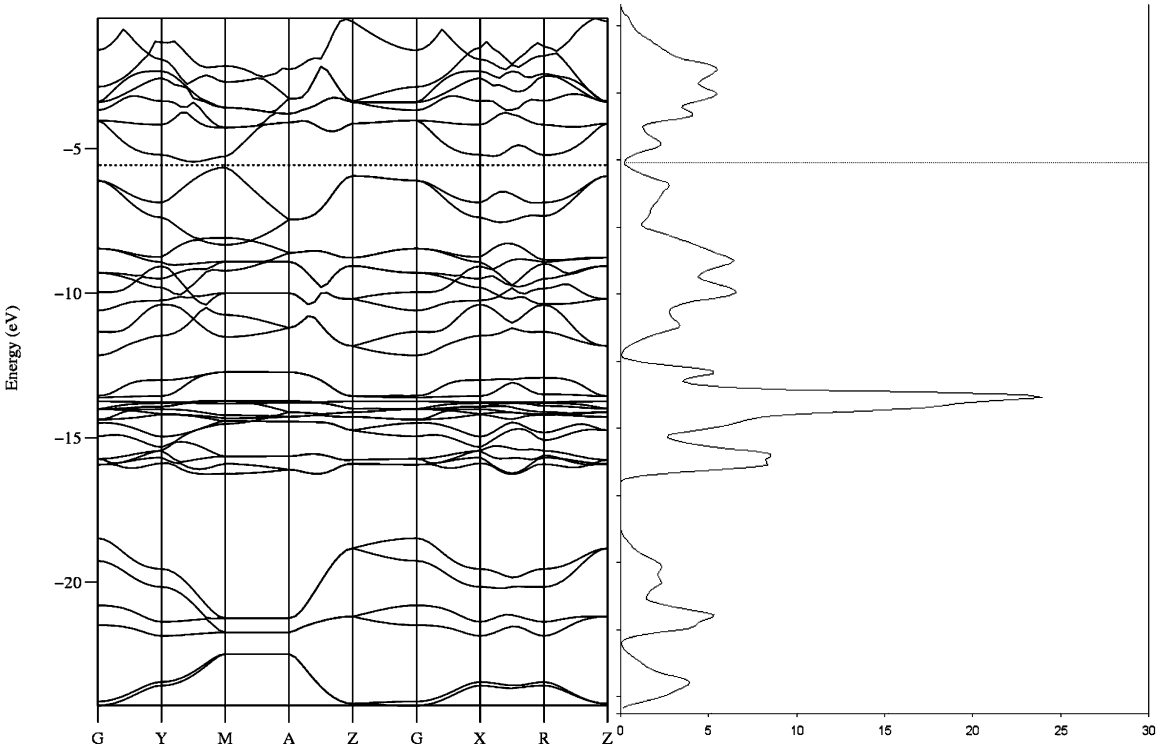

Figure 15. Bands and the total DOS of C_5Zn (**VII**).

An Isomer of C_5Zn without a C_{pt}

We have also explored an isomeric form of C_5M (**VII**) (M = Zn, Ni) with the tetrahedral and square planar atom identities interchanged relative to Figure 12 (Figure 14). Though square planar coordination around Zn is a rarity, there have been a few reports of these in the literature.[36] The resulting *P*42/*mmc* network has optimized lattice parameters given in Table 1. The *a* and *b* axes are considerably compressed owing to the shortening of the C_t-C_t bond to 129 pm (Table 1). The carbon skeletal pattern in this structure is entirely different; one way to think of the network is as an acetylenic complex of M (Figure 14). The C_t-C_t bond is much shorter compared to that of **V**, which shows the π-back-donation is not very strong with Zn. This is probably due to the very large differences in the orbital energies of Zn and C.

A comparison of the energies between the two forms of C_5Zn (**V** and **VII**) shows the latter (C in tetrahedral sites) to be more stable than the former one (Zn in tetrahedral sites) by an energy of 122 kJ mol^{-1} per C_5Zn unit. The band structure and total DOS of **VII** is given in Figure 15. The very small Fermi gap indicates that this structure is likely to be a semiconductor. The band structure of C_5Ni showed metallic behavior but a larger band gap compared to C_5Zn at an electron occupation appropriate to Zn. The EH calculation on the C sublattice alone also gave a definite band gap. This supports the perception of the carbon skeleton in this structure (see drawing in inset of Figure 14) being well described by a classical Lewis structure; hence Zn probably exists here in a zero oxidation state.

(36) Brock, S. L.; Kauzlarich, S. M. *Inorg. Chem.* **1994**, *33*, 2491.

Conclusions

C_5^{2-} is an interesting building block for potentially realizable 3D networks with C_{pt}, both with main group and transition elements. This paper is the first report on the theoretical design and hypothetical characterization of such a stable network. Theoretical studies on discrete systems containing C_5^{2-} units show two preferences in countercation coordination: (a) through the outer carbon lone pairs of the C_5^{2-} unit and (b) through the terminal carbons, but with the metal binding the two nonbonded C_t atoms. Among the two, the former is preferred in monomers based on the relative stabilities of the isomeric forms studied. We construct a variety of extended networks derived conceptually from the monomer and dimer models and using a simple model of the bonding capabilities of the C_5^{2-} unit. The hypothetical C_5M_x ($x = 1$, M = Pt, Zn, Be; $x = 2$, M = Li) systems proposed in this work in general have relatively large band gaps, suggesting semiconducting or insulating behavior.

Acknowledgment. We are grateful to the National Science Foundation for its support of the research at Cornell through Grant CHE-0204841, the Decanatura de Investigacion y Posgrado (DIP-UDLA), the Deutsche Forschungsgemeinschaft (DFG), and CONACYT (G34037-E and G32710-E) for financial support. G.M., A.V., and M.M.R. wish to thank Prof. Seifert and Dr. Heine (TU) for their kind comments and discussion.

Supporting Information Available: The computed energies, symmetries, and coordinates for all the reported systems, both molecular and extended. This material is available free of charge via the Internet at http://pubs.acs.org.

JA046405R